Experimental Study of Oscillation Behaviors in Confined Impinging Jets Reactor Under Excitation

Wei-Feng Li, Wen-Wei Qian, Guang-Suo Yu, Hai-Feng Liu, and Fu-Chen Wang
Key Laboratory of Coal Gasification and Energy Chemical Engineering of Ministry of Education, Energy Chemical Engineering Dept., East China University of Science and Technology, Shanghai 200237, China

Shanghai Engineering Research Center of Coal Gasification, East China University of Science and Technology, Energy Chemical Engineering Dept., Shanghai 200237, China

DOI 10.1002/aic.14617
Published online September 18, 2014 in Wiley Online Library (wileyonlinelibrary.com)

Dynamic behaviors in a three-dimensional confined impinging jets reactor (CIJR) under excitation were experimentally studied by a flow visualization technique at $75 \leq Re \leq 150$. The effects of inlet Reynolds numbers (Re), excitation frequencies and excitation amplitudes on the oscillation behaviors in CIJR have been investigated by a particle image velocimetry (PIV) and a high-speed camera. Results indicate that the excitation in the inflow of the opposed jets can induce periodic oscillation of the impingement plane along the axis, whose oscillation frequency is equal to the excitation frequency. At $Re \leq 100$, the induced axial oscillation can further cause a deflective oscillation with a frequency nearly equal to the excitation, and the scale of the vortex in the impingement plane is well regulated by the excitation frequency. At $Re = 150$, the excitation of amplitude less than 20% has insignificant effect on the deflective oscillation existing in CIJR. A semiempirical formula has been proposed to predict the oscillation amplitude of the impingement plane in CIJR under excitation. © 2014 American Institute of Chemical Engineers *AIChE J*, 61: 333–341, 2015
Keywords: confined impinging jets reactors, oscillation, excitation

Introduction

In the recent three decades, impinging jets have been widely and successfully applied to more and more industrial processes where mixing affects the final product distribution or quality, for example, fluids mixing, rapid chemical reaction, gasification, combustion, extraction, absorption, drying, and nanoparticle synthesis.[1] Most studies about the impinging jets reactor are about the T-jets mixer, reaction injection molding (RIM) and confined impinging jets reactors (CIJR) with miniscales or microscales. Typically, CIJR has two opposed nozzles with a diameter about 1 mm and operating Reynolds numbers are in the range of 50 to 600, and the flow regime and mixing mechanism are key issues for the scale-up and increasing industrial applications.[2]

The flow and mixing in CIJR have been intensively investigated in last three decades by means of flow visualization techniques, experimental measurements, numerical simulations, and theoretical analyses.[3–18] Many researchers have observed the transition from a segregated steady flow to a dynamic chaotic flow regime in CIJR at $Re > 100$, which is characterized by the formation of a pancake-like structure and the flow oscillates with a complex mode.[3–5,7–11] With increasing Reynolds numbers above the critical one, the flow in CIJR begins to show a more chaotic behavior.[6,11,15] In our recently published paper,[17] the flow regimes in CIJR were experimentally investigated at $100 \leq Re \leq 2000$ and $2 \leq D/d \leq 12$ (where D is the reactor diameter and d is the nozzle diameter). It has been indentified that with increasing Re, a segregated flow regime, a self-sustained deflective oscillation and a combination regime of vortex shedding and axial instability emerge in turns. The axial instability is characterized by an axial irregular oscillation along the axis, while the deflective oscillation is characterized by a regular S-shaped oscillation in the radial directions. The concurrence of radial deflective oscillation and axial oscillation is the main reason of the complex and chaotic flow in CIJR. However, the underlying mechanism and the internal relationship between the axial oscillation and radial deflective oscillation in CIJR still need further investigations.

In our previous study,[19,20] axisymmetric and planar opposed jets with modulated airflow or acoustic excitation have been experimentally studied. Results show the impingement plane of axisymmetric opposed jets synchronizes with the excitation and the oscillation amplitude decreases with the increase of the excitation frequency.[19] For planar opposed jets, the acoustic excitation of amplitude less than 30% has little effect on the self-sustained deflective oscillation.[20] Due to the effect of confined boundary of the reactor chamber, the flow regime in CIJR is largely different from unrestricted opposed jets, so the results obtained from unrestricted opposed jets with excitation cannot be directly applied in CIJR.

Additional Supporting Information may be found in the online version of this article.

Correspondence concerning this article should be addressed to W.-F. Li at liweif@ecust.edu.cn.

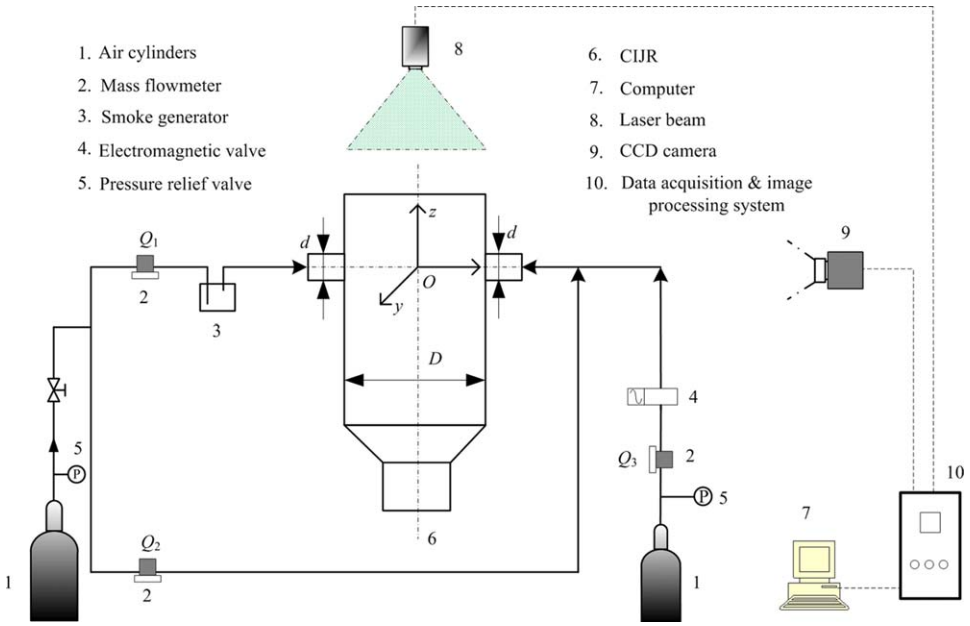

Figure 1. Schematic plan of experimental flowchart.

[Color figure can be viewed in the online issue, which is available at wileyonlinelibrary.com.]

The modulated inflow has been applied in active mixing devices such as T-shaped or Y-shaped micromixers.[21,22] Results show that when pulsed inflow is adopted in one jet or in two jets with a phase difference, the fluid mixing are remarkably enhanced.[23–26] However, more attention in these studies is focused on the effects of the pulsed inflow on the final mixing performance, and little emphasis has been put on the oscillation behaviors in the mixer chamber. Up to now, the fundamental study about the effects of pulsed inflow on the oscillation instability in CIJR or RIM is very rare, and the very few works that can be found in the literature are preliminary numerical simulations. Erkoç et al.[27] have performed numerical simulations to study the effect of pulsation with different frequencies on the flow dynamics of a two-dimensional laminar RIM. Simulation results show that the oscillation amplitude of the pulsation has a strong effect on the flow, and this effect increases with increasing amplitude up to the extreme case where the imposed pulsation completely drives the dynamics of the system. Icardi et al.[15,16] have investigated the flow field in CIJR by means of microPIV and Direct Numerical Simulation (DNS), and pointed out that oscillations present in the inflows have notable effects on the chaotic flow in the reactor, and some small excitation oscillations similar to the experimental ones should be introduced in inflow conditions in DNS. It can be seen that the disturbance in the inflows of the opposed jets significantly affects the flow dynamics in CIJR, which have not been revealed experimentally yet.

Motivated by the contributions of above studies, we present a fundamental experimental study of the oscillation behaviors in CIJR with pulsed inflow at $75 \leq Re \leq 150$ in this article. The effects of excitation amplitudes and frequencies on the oscillation behaviors in CIJR were investigated by a flow visualization technique combining a particle image velocimetry (PIV) system and a high-speed camera. Our objectives are to investigate the effects of the flux fluctuation on the oscillation instability in CIJR, and also to provide a flow dynamics controlling method for CIJR.

Experimental Methods

Experiment setup and flow visualization

The schematic plan of the experiment setup and flowchart is drawn in Figure 1. Air was supplied by an air cylinder after pressure reduction. The fluxes of the airflows to the nozzles were controlled by two mass flow meters (accuracy: $\pm 0.25\%$ of full-scale deflection (FSD), range: 0.3–20 L/min). The flow field of confined opposed jets was obtained by two identical opposing nozzles axisymmetrically installed on a cylindrical chamber. The instantaneous flow patterns in CIJR were visualized by the white smoke generated by some small fuming tablets. In the experiment, the smoke was introduced to the left jet to observe the impingement plane more clearly.

The slices of visualization images of the smoke-seeded flow were captured by the charge coupled device (CCD) camera of a PIV system (Dantec), and the pair of pictures was acquired with a frequency of 10 Hz. Due to the limitation of the frequency of the pulsed laser, the visualization images were also captured by a high-speed camera to analyze the movement of the impingement plane with a acquiring frequency of 1000 fps. The recorded digital images were analyzed by the NIH image freeware to obtain the oscillation frequencies or oscillation amplitudes of the dynamic behavior of the impingement plane in CIJR. The detailed method of the image processing can be found in our previous papers.[17,19]

As shown in Figure 1, the CIJR used for this experiment had a flat top and a conical constriction at the outlet and was made of acrylic material. The chamber diameter (D) was 50.00 ± 0.02 mm, and the dimensionless chamber diameter normalized by the nozzle exit diameter (D/d) was 4.8. The total height of the cylinder of CIJR was $2D$, and the height from nozzle plane to the dome was $0.5D$. The bulk mean velocities (u_0) at the nozzle exits were in the range of 0.11–0.21 m/s, and the corresponding jet Reynolds numbers ($du_0\rho/\mu$) were in the range of 75–150.

Excitation method

As shown in Figure 1, the pulsed airflow from another air cylinder was added to the base flow of left jet. The

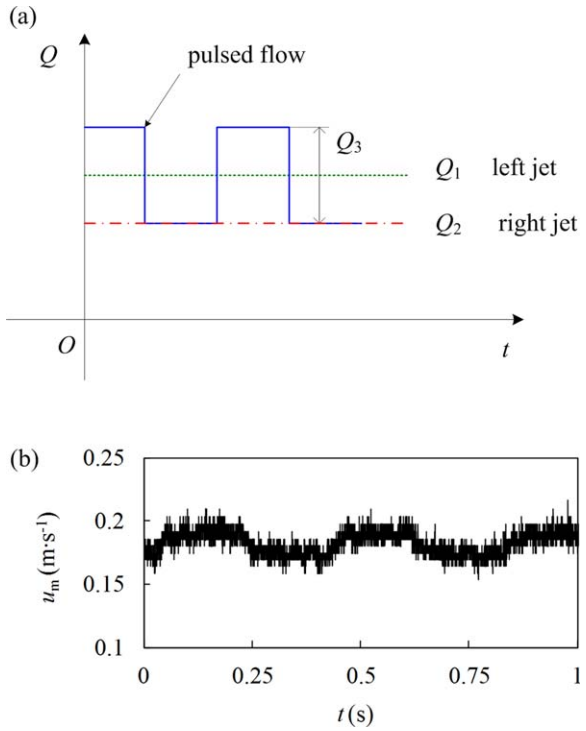

Figure 2. (a) Sketch map of the flow rate controlling of the opposed jets in CIJR with pulsation and (b) the instantaneous velocity fluctuation of modulated jet at $Re = 100$, $f_e = 2.5$ Hz, and $k = 10\%$.

[Color figure can be viewed in the online issue, which is available at wileyonlinelibrary.com.]

modulated airflow was generated and controlled by the periodic open and close of an electromagnetic valve with a very short response time (less than 5 ms) and a high frequency (up to 100 Hz). The excitation frequencies (f_e) were in the range of 1–20 Hz in this experiment. The excitation amplitude of the modulated airflow was controlled and regulated by a pressure relief valve and a mass flow meter (accuracy: ±0.25% of FSD, range: 0.03–2 L/min). The intermittent flow of the pulsed airflow was Q_3, and the mean flow rates of the base flows of the opposed jets were Q_1 and Q_2, respectively. The excitation amplitude was defined as the ratio of the pulsed airflow to the base flow ($k = Q_3/Q_1$) and was in the range of 5%–20%. The schematic of the flow control of the opposed jets and the pulsed flow is shown in Figure 2a. In the experiment, the momentum balance of the opposed jets in CIJR was adjusted according to the relationship of $Q_1 = Q_2 + \overline{Q_3}$. The velocity fluctuation on the axis of the excited jet (u_m) was measured at the nozzle exit by a hot-wire anemometer (Dantec) with an acquiring frequency of 10 kHz. The time series of the velocity fluctuation of the modulated jet at $Re = 100$, $f_e = 2.5$ Hz, and $k = 10\%$ is shown in Figure 2b. It can be seen that the time series generally displays a square-wave shape, and its frequency and amplitude are just equal to those of the excitation.

Results

Flow visualization images of flow patterns

Some typical instantaneous slices of smoke-seeded flow patterns captured by the CCD camera of the PIV system in CIJR without excitation are presented in Figure 3, and three distinct flow regimes are identified for $Re = 75$, 100, and 150. A stable segregated flow can always be observed at $Re = 75$ (animation M1 of Supporting Information). About at $Re = 100$, the center part of the impingement plane is stable and exhibits a segregated flow regime but the outer parts flap periodically (animation M2 of Supporting Information). About at $Re = 150$, a flow regime characterized by the deflective oscillation of the impingement plane with a regular period is identified (animation M3 of Supporting Information). The segregated flow regime, the flapping oscillation and the radial deflective oscillation at $Re = 75$, 100, and 150 are corresponding to a stable state, a transitional state and an oscillation instability state of the flow dynamics in CIJR, and we chose these three typical Reynolds numbers to investigate the effects of the excitation on the flow dynamics in CIJR.

The typical visual images of flow patterns in CIJR with excitation at $Re = 75$ and 100 are shown in Figures 4 and 5. Results indicate that a periodic axial oscillation and some vortex structures in the impingement plane emerge in CIJR with pulsation. It can be seen from Figure 4 that the amplitude of the axial oscillation and the scale of the vortex structure decrease with increasing excitation frequency, and the excitation of $f_e > 5$ Hz has insignificant effect on the flow in CIJR. Figure 5 shows that the slight excitation of $k = 5\%$ only causes a small axial oscillation and a flapping oscillation of the outer parts of the impingement plane. For $k = 10\%$ and 20%, the low-frequency excitation of $f_e < 2.5$ Hz can induce a combination of an axial periodic oscillation and radial deflective oscillation of the impingement plane (animation M4 of Supporting Information). At $2.5 \le f_e < 10$ Hz, the amplitude of the axial oscillation caused by the pulsed inflow decreases significantly, but some regular vortex rings appear in the impingement plane (animation M5 of Supporting Information). At $f_e > 10$ Hz, the excitation has insignificant effect on the flow in CIJR at $Re = 100$. Generally, the oscillation amplitude and range of the response frequency of the impingement plane to the excitation increase with exit Reynolds numbers and excitation amplitudes.

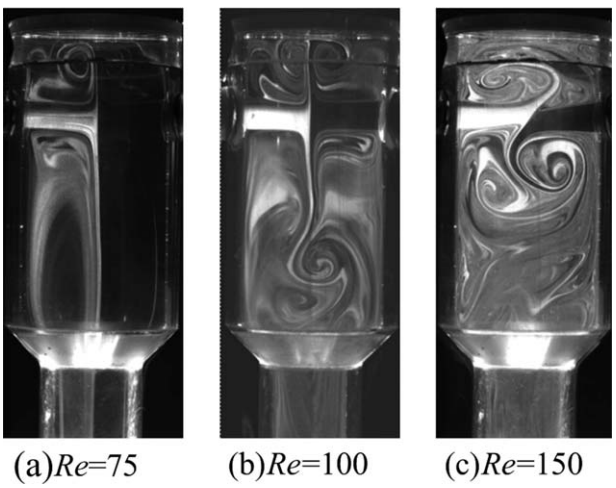

Figure 3. Typical visual images in CIJR without excitation.

(a) $Re = 75$, (b) $Re = 100$, and (c) $Re = 150$.

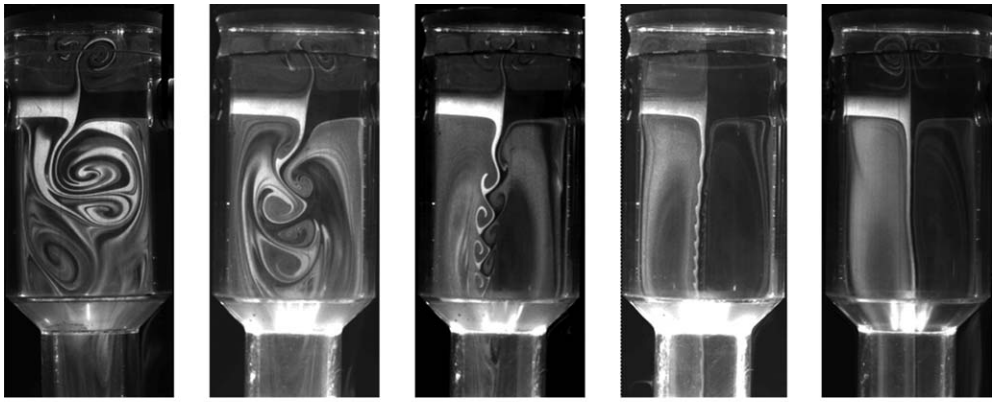

Figure 4. Typical visual images in CIJR with pulsation at *Re* = 75 and *k* = 20%.

(a) f_e = 0.5 Hz, (b) f_e = 1 Hz, (c) f_e = 2.5 Hz, (d) f_e = 5 Hz, and (e) f_e = 10 Hz.

The typical visual images of flow patterns in CIJR under excitation at $Re = 150$ and $k = 20\%$ are shown in Figure 6. It can be observed that the impingement plane still shows a deflective oscillation similar to the case without excitation. Meanwhile, the impingement plane displays an axial oscillation caused by the pulsed inflow, and thus, the impingement plane exhibits a hybrid mode of axial periodic oscillation and radial deflective oscillation (animation M6 of Supporting Information). Results show that for the cases of $k = 5$ and 10%, the deflective oscillation of the impingement plane is still regular despite the axial oscillation. With increasing excitation amplitudes of $k \geq 20\%$, the large axial oscillation

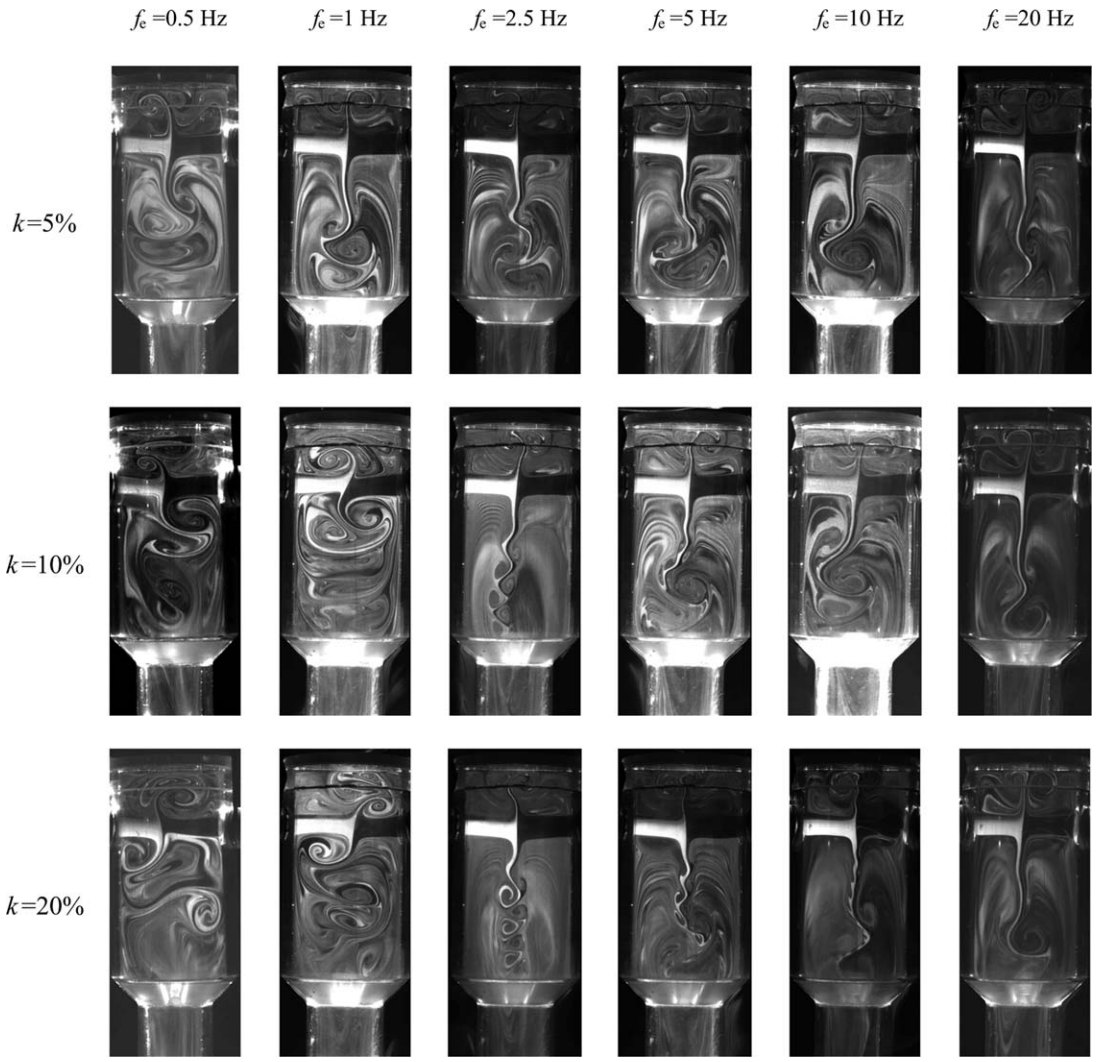

Figure 5. Typical visual images in CIJR under excitation at *Re* = 100.

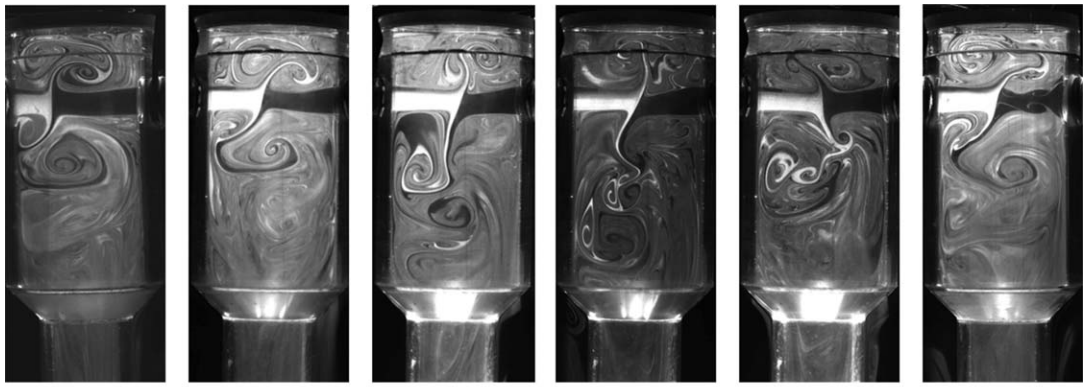

Figure 6. Typical visual images in CIJR with excitation at *Re* = 150 and *k* = 20%.

(a) f_e = 0.5 Hz, (b) f_e = 1 Hz, (c) f_e = 2.5 Hz, (d) f_e = 5 Hz, (e) f_e = 10 Hz, and (f) f_e = 20 Hz.

becomes to affect the deflective oscillation and the flow in CIJR exhibits a complex hybrid oscillation.

Axial oscillation of the impingement plane under excitation

The time series of impingement point on the axis during the axial oscillation in CIJR at $Re = 150$ and $k = 20\%$ are presented in Figure 7, in which the values at $f_e > 1$ Hz are analyzed from the images captured by the high-speed camera, and those at $f_e \leq 1$ are analyzed from the images recorded by the CCD camera of the PIV system. Results indicate that in the absence of excitation, the impingement plane exhibits a low-frequency and irregular oscillation on the axis, as shown in Figure 7a. With the pulsed inflows, the movement of the impingement plane displays an axial periodic oscillation. Figure 8 presents the oscillation

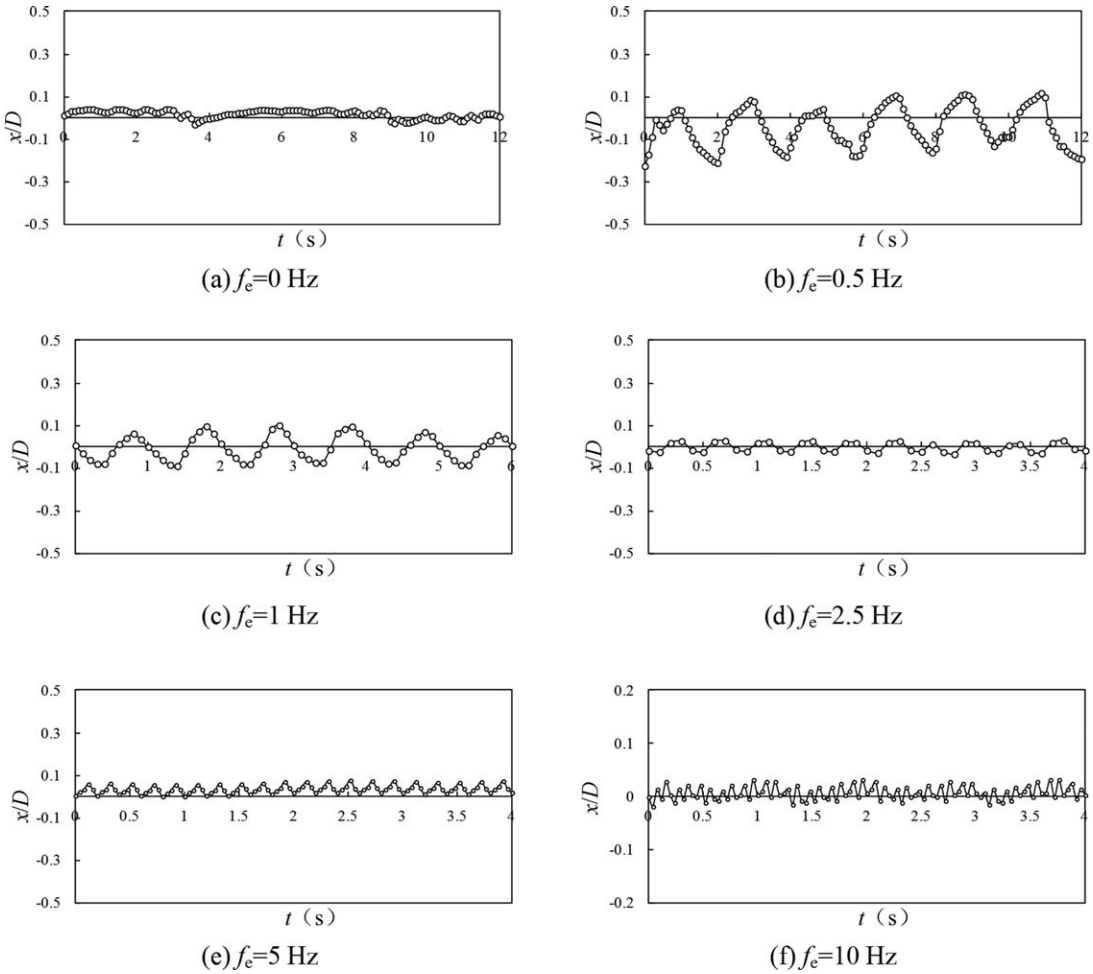

Figure 7. Time series of impingement point on the axis during the axial oscillation in CIJR under excitation at *Re* = 150 and *k* = 20%.

(a) f_e = 0 Hz, (b) f_e = 0.5 Hz, (c) f_e = 1 Hz, (d) f_e = 2.5 Hz, (e) f_e = 5 Hz, and (f) f_e = 10 Hz.

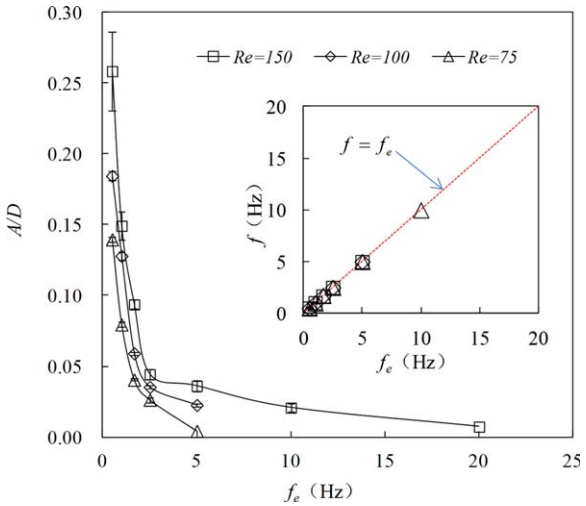

Figure 8. Oscillation frequencies and amplitudes of impingement plane in CIJR under excitation at k=20%.

[Color figure can be viewed in the online issue, which is available at wileyonlinelibrary.com.]

frequencies (f) and amplitudes (A) of the axial oscillation of the impingement planes at $k = 20\%$, in which each value is the average analyzed from 15 oscillation periods, and the error bars mark the standard deviations. The figure shows that the oscillation amplitudes of the impingement planes decrease rapidly with the increase of excitation frequencies, and increase with jet Reynolds numbers at a given excitation frequency. Results in the figure also indicate that the oscillation frequencies of axial oscillation are equal to the excitation frequencies, and the response frequencies of the impingement plane to the excitation are less than 10 Hz and the ranges are expanded with increasing jet Reynolds numbers.

When the oscillation amplitudes under all experimental conditions are normalized by $\frac{1}{2}u_0 \cdot k$, the experimental results at various Re and excitation amplitudes are found to be overlapped near a curve, as shown in Figure 9, which indicates

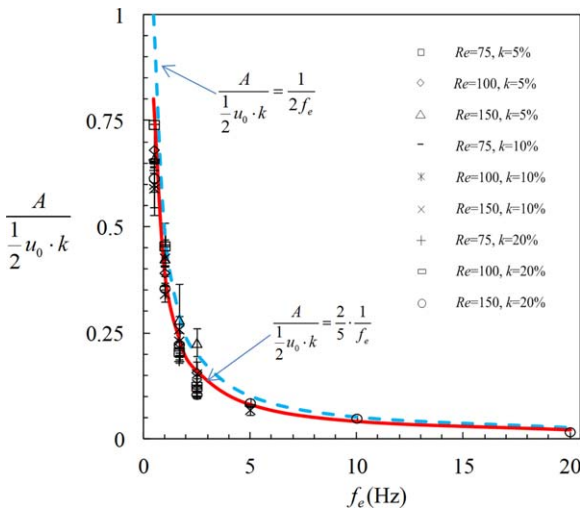

Figure 9. Normalized amplitudes of axial oscillation in CIJR with excitation.

[Color figure can be viewed in the online issue, which is available at wileyonlinelibrary.com.]

the axial oscillation amplitude is approximately proportional to the product of u_0 and k.

According to the experimental results in our previous study,[19] the mean movement speed of the impingement plane (u_{ip}) with excitation is equal to or less than the velocity difference of axisymmetric opposed jets. As shown in Figure 2a, $\frac{1}{2}u_0 \cdot k$ is the instantaneous velocity difference of the opposed jets in CIJR under excitation, so the average movement speed of the impingement plane can be described as

$$u_{ip} \leq \frac{1}{2}u_0 \cdot k \tag{1}$$

If the oscillation amplitude is less than the chamber diameter, the oscillation amplitude of the impingement plane under excitation is equal to the moving distance in half an oscillation period. It can be seen from Figure 8 that this prerequisite is satisfied in this study, and thus, the following equation can be used to describe the oscillation amplitude of the impingement plane in CIJR under excitation

$$A = \frac{u_{ip}}{2f_e} \tag{2}$$

Substituting Eq. 1 in Eq. 2, then we get

$$A \leq \frac{\frac{1}{2}k \cdot u_0}{2f_e} \quad \text{or} \quad \frac{A}{\frac{1}{2}k \cdot u_0} \leq \frac{1}{2f_e} \tag{3}$$

If we presume $u_{ip} = \frac{1}{2}u_0 \cdot k$, then Eq. 3 can be written as

$$\frac{A}{\frac{1}{2}k \cdot u_0} = \frac{1}{2f_e} \tag{4}$$

The curve corresponding to Eq. 4 is plotted as the dashed line in Figure 9. It can be seen that the equation predicts the trend of the experimental values, but the prediction values are somewhat larger than the experimental ones.

Due to the inlet velocity fluctuation of the opposed jets, as shown in Figure 2b, the actual movement speed will be less than $\frac{1}{2}u_0 \cdot k$, and the oscillation amplitude of the impingement plane will decrease consquently.[19] To be more precise, the movement velocity can be analyzed from the time series of the locations of the impingement point during the oscillation as shown in Figure 7. Results reveal that the ratio of u_{ip} to $\frac{1}{2}u_0 \cdot k$ is about in the range of 0.7–0.9. If an average value of 0.8 is chosen, that is, $u_{ip} = 0.8 \cdot \frac{1}{2}u_0 \cdot k = \frac{2}{5}u_0 \cdot k$, then Eq. 3 is modified as

$$\frac{A}{\frac{1}{2}u_0 \cdot k} = \frac{2}{5} \cdot \frac{1}{f_e} \tag{5}$$

The curve corresponding to Eq. 5 is also plotted in Figure 9. It can be seen that the predictions by the modified equation are in good agreement with the experimental results.

Deflective oscillation of the impingement plane under excitation

The frequencies of the deflective oscillation in CIJR with and without excitation are presented in Figure 10. It can be seen from Figure 10a that at $Re = 75$ and $f_e < 5$ Hz the oscillation frequencies of the impingement plane is exactly equal to the excitation frequency, and there is no oscillation at $f_e \geq 5$ Hz. For $Re = 100$, the frequency range in response to the excitation expands with increasing excitation amplitudes. When the impingement plane cannot response to the excitation, its frequency is about 0.66 Hz, which is nearly equal to

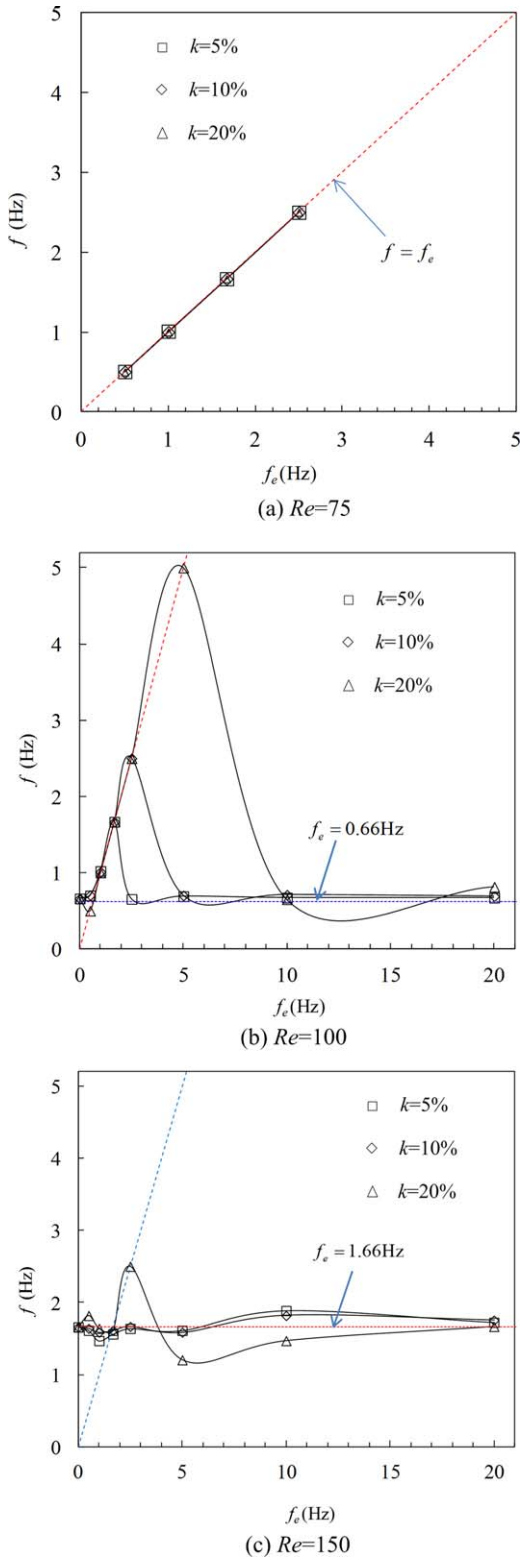

Figure 10. Frequencies of deflective oscillation in CIJR with and without excitation.

(a) $Re = 75$, (b) $Re = 100$, and (c) $Re = 150$. [Color figure can be viewed in the online issue, which is available at wileyonlinelibrary.com.]

the flapping frequency without excitation, as shown in Figure 10b. It is interesting to see that at $Re = 150$ and $k < 20\%$ the frequencies of the deflective oscillation nearly keep invariable and are around the line of $f = 1.66$ Hz, which is corresponding to the frequency of the deflective oscillation without excitation, as shown in Figure 10c. At $k = 20\%$, the excitation starts to affect the inherent deflective oscillation in CIJR, especially at $f_e = 2.5$ Hz. Results in Figure 10c indicate that the deflective oscillation is not subject to the excitation of $k < 20\%$, which means the fluctuation in the inflow is not the dominant cause of the deflective oscillation observed in CIJR.

Discussion

Study of the oscillation behaviors in CIJR with excitation is important to understand the intrinsic flow regimes, as the pulsed inflow can be seen as a periodic disturbance imposed on the flow system. Results in these experiments indicate that the excitation in the inflow of the opposed jets can induce a periodic axial oscillation of the impingement plane, whose frequency is just equal to the excitation frequency. At $Re < 100$, the induced axial oscillation can further cause a deflective oscillation with a frequency approximately identical to the excitation frequency, and flow in CIJR displays a hybrid of axial oscillation and radial deflective oscillation. Results also indicate that the scales of the vortex structures in CIJR are well determined by the excitation frequency, and show a direct relevance with the axial oscillation amplitude. At $Re = 150$, the deflective oscillation nearly keeps invariable and is not affected by the excitation of $k < 20\%$. It should be noted that the induced deflective oscillation at $Re \leq 100$ is distinct to the self-sustained deflective oscillation at $Re = 150$, as the former is mainly induced by the axial oscillation which is caused by the excitation of the pulsed inflow, but the latter is mainly determined by the interaction of the impingement plane and the confined wall of chamber.[17] Results in this study prove that the axial oscillation is caused by the inflow fluctuation in the opposed jets in CIJR while the deflective oscillation is a kind of self-sustained oscillation.[17,19,20]

The results in this study can be used to explain the self-sustainable oscillation and chaotic flow regime in CIJR in the literature. At $Re < 100$, the fluctuation in the jets is very low, and thus cannot cause an axial oscillation, and a separated flow regime appears in CIJR. As Re increases to 100 or larger, the fluctuation in the inflow grows and induces random axial oscillation, whose frequency and amplitude increase with Re. Meanwhile, the jet instability, the impinging instability in the stagnation region, and especially the interaction between the impingement plane and the confined chamber wall will cause a self-sustained deflective oscillation.[3–5,10,17] About at $Re > 300$, the random axial oscillation increases largely, and therefore, the concurrence of the random axial oscillation and the deflective oscillation makes the flow in CIJR display a chaotic flow regime.[6,11,15] As the fluctuation levels of the inflows in CIJR in various experiments in the literature are different, the reported critical Reynolds number for the onset of the oscillation and the oscillation behavior have some discrepancies. These results indicate the flow in CIJR is very instable, and the disturbance in the inflows must be considered in the experiment. Just as Icardi et al.[15,16] have pointed out, in the numerical simulations of the flow dynamics or the mixing in CIJR, the unsteady solver and inflow conditions considering the fluctuation are preferable for this unsteady and complex flow.

These experiments prove that imposing pulsed inflow is a very effective method to excite the oscillation in CIJR, with which the scales of the vortex structures can also be well regulated by the excitation frequency and amplitude. This excitation method has some reference significance to active mixing and process intensification in CIJR, especially for the case of low operating Reynolds number. It should be pointed out that the response frequency of the excitation is in the range of 0–10 Hz due to the low inlet velocities in this experiments. According to Eq. 5, the oscillation amplitude of the axial oscillation caused by the excitation in CIJR is inversely proportional to the excitation frequency, but is proportional to the jet Reynolds number and the excitation amplitude. One can deduce from empirical equation that with the increase of inflow velocities or excitation amplitudes the response frequency will increase consequently.

Conclusions

To further disclose the flow regimes and exploit a method of mixing intensification of impinging jets for engineering applications, it is very necessary to study the oscillation behaviors in CIJR under excitation. In this study, the oscillations behaviors in CIJR with pulsed inflow at $75 \leq Re \leq 150$ were investigated by a flow visualization technique and a flow exciting method. Results indicate that the excitation in the inflow of the opposed jets in CIJR can induce a periodic axial oscillation of the impingement plane, whose oscillation frequency is just equal to the excitation frequency. A semiempirical formula has been proposed to predict the oscillation amplitude of the impingement plane in CIJR under excitation. At $Re \leq 100$, the induced axial oscillation can further cause a deflective oscillation with a frequency similar to the excitation frequency, and the scales of the vortex structures in CIJR are well determined by the excitation frequency and amplitude. At $Re = 150$, the excitation also excites an axial oscillation, but it has insignificant effect on the frequency of the deflective oscillation existing in CIJR at $k < 20\%$. These results indicate that in the experiment or numerical simulation of the flow dynamics in CIJR, the fluctuation in the inflows of the opposed jets must be considered.

This study presents a significant contribution to the knowledge of the intrinsic mechanism of the oscillation instability in CIJR, also provides some principles to excite or control the dynamics behaviors in CIJR. The results are also instructive for the future computational fluid dynamics simulation and stability analysis of the CIJR.

In future study, detailed measurement and assessment of the mixing quality will be conducted by PLIF in CIJR with pulsed inflow of liquid.

Acknowledgments

This study was supported by the National Development Programming of Key Fundamental Researches of China (2010CB227004). Especially, we express our sincere thanks to the anonymous reviewers for their helpful suggestions on the quality improvement of the paper.

Notation

A = oscillation amplitude
d = jet diameter or nozzle inner diameter
D = chamber diameter
f = oscillation frequency
k = ratio of the pulsed flow to the base flow
Q = bulk flux
Re = jet Reynolds number
t = time
u = velocity
x, y, z = three-dimensional coordinates
ρ = air density
μ = dynamic viscosity of air

Literature Cited

1. Tamir A. *Impinging Streams Reactors: Fundamentals and Applications*. Amsterdam: Elsevier, 1994.
2. Santos RJ, Sultan MA. State of the art of mini/micro jet reactors. *Chem Eng Technol*. 2013;36:937–949.
3. Wood PE, Hrymak A, Yeo R, Johnson DA, Tyagi A. Experimental and computational studies of the fluid mechanics in an opposed jet mixing head. *Phys Fluids A*. 1991;3:1362–1368.
4. Zhao Y, Brodkey RS. Averaged and time-resolved, full-field (three-dimensional), measurements of unsteady opposed jets. *Can J Chem Eng*. 1998;76:536–545.
5. Johnson DA, Wood PE. Self-sustainable oscillations in opposed impinging jets in an enclosure. *Can J Chem Eng*. 2000;78:867–875.
6. Unger DR, Muzzio FJ. Laser-induced fluorescence technique for the quantification of mixing in impinging jets. *AIChE J*. 1999;45:2477–2486.
7. Teixeira AM, Santos RJ, Costa MRPFN, Lopes JCB. Hydrodynamics of the mixing head in RIM: LDA flow-field characterization. *AIChE J*. 2005;51:1608–1619.
8. Santos RJ, Teixeira AM, Lopes JCB. Study of mixing and chemical reaction in RIM. *Chem Eng Sci*. 2005;60:2381–2398.
9. Li X, Santos RJ, Lopes JCB. Modelling of self-induced oscillations in the mixing head a RIM machine. *Can J Chem Eng*. 2007;85:45–54.
10. Santos RJ, Erkoç E, Dias MM, Teixeira AM, Lopes JCB. Hydrodynamics of the mixing chamber in RIM: PIV flow-field characterization. *AIChE J*. 2008;54:1153–1163.
11. Santos RJ, Erkoç E, Dias MM, Lopes JCB. Dynamic behavior of the flow field in a RIM machine mixing chamber. *AIChE J*. 2009;55:1338–1351.
12. Johnson BK, Prud'homme RK. Chemical processing and micromixing in confined impinging jets. *AIChE J*. 2003;49:2264–2282.
13. Liu Y, Fox RO. CFD predictions for chemical processing in a confined impinging-jets reactor. *AIChE J*. 2006;52:731–744.
14. Gavi E, Marchisio DL, Barresi AA. CFD modelling and scale-up of Confined Impinging Jet Reactors. *Chem Eng Sci*. 2007;62:2228–2241.
15. Icardi M, Gavi E, Marchisio DL, Barresi AA, Olsen MG, Fox RO, Lakehal D. Investigation of the flow field in a three-dimensional Confined Impinging Jets Reactor by means of microPIV and DNS. *Chem Eng J*. 2011;166:294–305.
16. Icardi M, Gavi E, Marchisio DL, Olsen MG, Fox RO, Lakehal D. Validation of LES predictions for turbulent flow in a Confined Impinging Jets Reactor. *Appl Math Model*. 2011;35:1591–1602.
17. Li WF, Du KJ, Yu GS, Liu HF, Wang FC. Experimental study of flow regimes in three-dimensional confined impinging jets reactor. *AIChE J*. 2014;60:3033–3045.
18. Schwertfirm F, Gradl J, Schwarzer HC, Peukert W, Manhart M. The low Reynolds number turbulent flow and mixing in a confined impinging jet reactor. *Int J Heat Fluid Flow*. 2007;28:1429–1442.
19. Li WF, Huang GF, Tu GY, Liu HF, Wang FC. Experimental study of oscillation of axisymmetric turbulent opposed jets with modulated airflow. *AIChE J*. 2013;59:4828–4838.
20. Li WF, Huang GF, Tu GY, Liu HF, Wang FC. Experimental study of planar opposed jets with acoustic excitation. *Phys Fluids*. 2013;25:014108.
21. Hessel V, Löwe H, Schönfeld F. Micromixers-a review on passive and active mixing principles. *Chem Eng Sci*. 2005;60:2479–2501.
22. Lee CY, Chang CL, Wang YN, Fu LM. Microfluidic mixing: a review. *Int J Mol Sci*. 2011;12:3263–3287.
23. Glasgow I, Aubry N. Enhancement of microfluidic mixing using time pulsing. *Lab Chip*. 2003;3:114–120.

24. Ito Y, Komori S. A vibration technique for promoting liquid mixing and reaction in a microchannel. *AIChE J*. 2006;52:3011–3017.
25. Sun CL, Sie JY. Active mixing in diverging microchannels. *Microfluid Nanofluid*. 2010;8:485–495.
26. Okkels F, Tabeling P. Spatiotemporal resonances in mixing of open viscous fluids. *Phys Rev Lett*. 2004;92:038301.
27. Erkoç E, Santos RJ, Dias MM, Lopes JCB. Enhancing the RIM process with pulsation technology: CFD study. In: Proceedings of European congress of chemical engineering (ECCE-6). Copenhagen, 16–20 September, 2007.

Manuscript received Apr. 20, 2014, and revision received Aug. 12, 2014.